Postprint of: Piotrowski R., Ujazdowski T. (2020) Model of Aeration System at Biological Wastewater Treatment Plant for Control Design Purposes. In: Bartoszewicz A., Kabziński J., Kacprzyk J. (eds) Advanced, Contemporary Control. Advances in Intelligent Systems and Computing, vol 1196. Springer, Cham. https://doi.org/10.1007/978-3-030-50936-1_30

Model of aeration system at biological wastewater treatment plant for control design purposes

Piotrowski R., Ujazdowski T.

Faculty of Electrical and Control Engineering, Gdańsk University of Technology, Gdansk, Poland,
robert.piotrowski@pg.gda.pl, ✉ tomek-ujazdowski@wp.pl

Abstract. The wastewater treatment plant (WWTP) is a dynamic, very complex system, in which the most important control parameter is the dissolved oxygen (DO) concentration. The air is supplied to biological WWTP by the aeration system. Aeration is an important and expensive activity in WWTP. The aeration of sewage fulfils a twofold role. Firstly, oxygen is provided as the main component for biological processes. Secondly, it supports mixing the sludge with the delivered sewage, which helps to treat the sewage. The paper proposes a model of the aeration system for biological WWTP located in Northeast Poland. This aeration system consists of the blowers, the main collector pipeline, three lines of the aeration with different diameters and lengths and diffusers. This system is a nonlinear dynamic system with faster dynamics compared to the internal dynamics of the DO at the biological WWTP. Control of the aeration system is also difficult in terms of control of the DO. A practical approach to model identification and validation is proposed. Simulation tests for aeration system at Matowskie Pastwiska WWTP are presented.

Keywords: aeration system, modelling, nonlinear system, wastewater treatment plant

1 Introduction

Wastewater treatment plays a key role for humanity. The waste entering lakes, rivers, and seas deteriorates the daily quality of life. Therefore, it is very important to improve the efficiency of wastewater treatment.

Batch type wastewater treatment plant (WWTP) (named Sequencing Batch Reactor – SBR) is a complex control system due to nonlinear dynamics, large uncertainty, multiple time scales in the internal process dynamics and multivariable structure. In addition, limited measurements are possible during plant operation. In the SBR, all biochemical processes occur in one tank, in the predefined sequence. SBR is a fill-and-draw activated sludge treatment system. This technology is widely used under small wastewater inflow conditions and may be designed using a single tank or a system of multiple tanks working in parallel. A usual work cycle involves following operational phases: filling, biological reactions (aerobic, anaerobic), sedimentation, decantation, and idling[1].

The oxygen is delivered into the SBR by the aeration system composed of blowers, pipes, valves, and diffusers. Aeration is an important and expensive activity in WWTP. The aeration of sewage fulfils a twofold role. Firstly, oxygen is provided as a main component for biological processes (denitrification, nitrification, phosphorus removal). Secondly, it supports mixing the sludge with the delivered sewage, which helps to treat the sewage. Insufficient amounts of oxygen interfere with the proper course of biological processes. At the same time, an excessively high oxygen level does not act profitably either. It does not improve the effectiveness of biological processes while producing higher costs of sewage treatment due to a longer time of aerating.

The variable which is directly related to sewage aeration is the dissolved oxygen (DO) concentration. DO control is important for WWTP energy efficiency. The total energy consumed by aeration processes is the factor deciding about total energy consumption in WWTP (above 50% of total operational cost) [2]. Previous research works presented various algorithms of DO control, e.g. [3-14].

The remainder of this paper is organized as follows. The case study aeration system is described in section 2. Model creation, structure presentation and subsystem division are presented in section 3. The results analysis and verification tests are illustrated in section 4. Section 5 concludes the paper.

2 Description of the aeration system

WWTP at Matowskie Pastwiska was modernized in 2018. The entire aeration system has changed and a new DO control system has been introduced. WWTP is composed of two identical, independently operating SBRs. Each of them is equipped with a separate aeration system which consists of a blower, diffuser system and pipeline. The required DO level is maintained by the variable speed blower. Blower airflow can be controlled within the range of 150 - 320 m^3/h. The pumped airflow moves into a pipeline and splits to tube diffuser systems located at the bottom floor of the SBR.

The pipeline consists of the main pipeline with a diameter of 104 mm and a length of the first part (horizontal) equal to 75.6 m and a second (vertical) 6 m that passes into a collector with a diameter of 154 mm and a length of 13 m. 6 branches depart from it (each with a diameter of 69 mm and 5.6 m long) supplying medium to distribution pipes (80 mm x 80 mm x 5 m). Fig. 1 shows the pipeline layout. The blower station is located on the left side of the pipeline, at the end of a 75 meter pipe. The diffuser system is located at the end of six branches. The diffusers are membrane tube type. There are 84 diffusers, separated 14 per branch spread over the entire surface of the SBR. The SBR has dimensions of 14 m length, 5.6 m width and 6 m height. The maximum fill level of the SBR is 5.5 m, while the minimum is 4 m. The level implies a hydrostatic pressure in the tank.

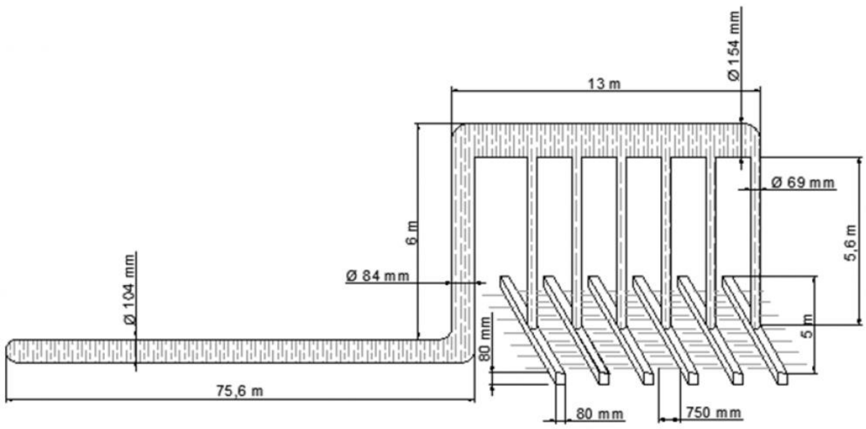

Fig. 1. Schematic diagram of the pipeline.

3 Modelling and parameters identification

3.1 Model structure

The general methodology of aeration system modelling was presented in [14]. The theoretical knowledge, manufacturer data records from case study plant and documentation characteristics of the system elements were applied. The structure of the model was based on a proven approach using an electric analog. This allows processes related to gas flows to be presented in a simpler way. The circuit is shown in Fig. 2. There are three main subsystems in the model: blowers, pipeline and aeration segment units. The blower is represented as a nonlinear current source and is accompanied by the designations - Q_b, Δp_b. Hydrostatic pressure is shown as a voltage source with a pressure drop Δp_h. Resistor R_c corresponds to the total unit pressure losses along the pipeline length, R_z losses resulting from changes in pipe diameter. The pipeline is presented as total fluid-flow capacitance C_c and p_c node. The aeration segment units are described by R_d resistance and C_d capacity. The pressure loss across diffuser is represented as Δp_d.

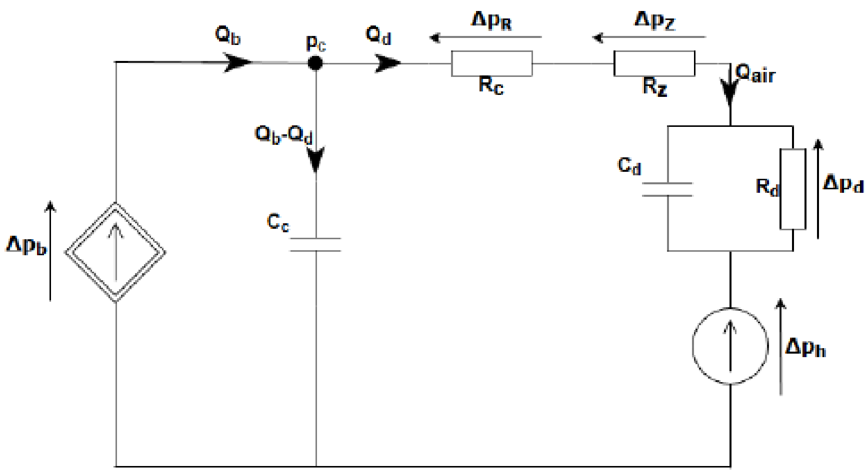

Fig. 2. Electrical analogy of the aeration system model.

3.2 Blowers

The blower station compresses air assuring appropriate pressure p_c at the pipeline. The blower operation was modelled based on the characteristics provided by the blower manufacturer. Using the characteristics, three matrices were created: characteristic velocities (Table 1), airflows (Table 2) and pressures (Table 3). The input parameters of the algorithm representing the operation of the blower are pressure p_c and blower rotational speed n. Based on them, the algorithm selects the appropriate mass airflow at the output. The values between the intervals are calculated as a weighted average of two adjacent values.

The blower model is represented as a nonlinear function:

$$Q_b = f\,(p_c\,,\,n) \tag{1}$$

where Q_b, p_c, n are the blower output airflow, pressure drop across the blower and motor rotational speed, respectively.

The use of a matrix to build a blower model allows for model adaptation depending on the type of blower in WWTP. The size of the characteristic pressure matrix (Table 3) is related to the use of other types of blowers in previous studies [15]. In order to preserve the universal character of the blower model, no matrix simplifications were applied.

Table 1. Matrix of blower characteristic velocities - **N**

column index and values (n [rpm])										
1	2	3	4	5	6	7	8	9	10	11
3000	3200	3400	3600	3800	4000	4200	4400	4600	4800	5000

Table 2. Matrix of blower characteristic airflows – **B**

B		column index and values (Q_b [Nm^3/hm])										
		1	2	3	4	5	6	7	8	9	10	11
row index and values	1	186.0	202.2	218.4	234.6	250.8	267.0	283.2	299.4	315.6	331.8	348.0
	2	182.4	198.6	214.8	231.0	247.2	263.4	279.6	295.8	312.0	328.2	344.4
	3	178.2	194.4	210.6	226.8	243.0	259.2	275.4	291.6	307.8	324.0	340.2
	4	174.6	190.8	207.0	223.2	239.4	255.6	271.8	288.0	304.2	320.4	336.6
	5	169.8	186.0	202.2	218.4	234.6	250.8	267.0	283.2	299.4	315.6	331.8
	6	166.2	182.4	198.6	214.8	231.0	247.2	263.4	279.6	295.8	312.0	328.2
	7	163.8	180.0	196.2	212.4	228.6	244.8	261.0	277.2	293.4	309.6	325.8
	8	157.2	173.4	189.6	205.8	222.0	238.2	254.4	270.6	286.8	303.0	319.3

Table 3. Matrix of blower characteristic pressures – P

P		column index and values (p_c [kPa])										
		1	2	3	4	5	6	7	8	9	10	11
row index and values	1	30	30	30	30	30	30	30	30	30	30	30
	2	35	35	35	35	35	35	35	35	35	35	35
	3	40	40	40	40	40	40	40	40	40	40	40
	4	45	45	45	45	45	45	45	45	45	45	45
	5	50	50	50	50	50	50	50	50	50	50	50
	6	55	55	55	55	55	55	55	55	55	55	55
	7	60	60	60	60	60	60	60	60	60	60	60
	8	70	70	70	70	70	70	70	70	70	70	70

The current rotational speed and pressure are compared with the table of characteristic values and the nearest elements marked as index are selected. The rotational speed proportionality (k_n) coefficient is obtained according to equation:

$$k_n = \frac{n - \boldsymbol{N}(j_n)}{\boldsymbol{N}(j_n + 1) - \boldsymbol{N}(j_n)} \tag{2}$$

where j_n is the column number of the N matrix with less or equal rotational speed. Intermediate pressure values can be expressed as:

$$\boldsymbol{p_i} = \boldsymbol{P}\,(j_n) + k_n \cdot (\boldsymbol{P}\,(j_n + 1) - \boldsymbol{P}\,(j_n)) \tag{3}$$

Intermediate airflow values are obtained from a similar relationship:

$$\boldsymbol{f_i} = \boldsymbol{B}\,(j_n) + k_n \cdot (\boldsymbol{B}\,(j_n + 1) - \boldsymbol{B}(j_n)) \tag{4}$$

To obtain the final value of the airflow at the blower, the pressure proportionality coefficient is calculated:

$$k_p = \frac{p_c - \boldsymbol{p_i}(j_f)}{\boldsymbol{p_i}(j_f + 1) - \boldsymbol{p_i}(j_f)} \tag{5}$$

where j_f is an element of the flow matrix with less or equal pressure from the **P** matrix.

Finally, the output value of the airflow Q_b is described by the following equation:

$$Q_b = \boldsymbol{f_i}(j_f) + k_p \cdot (\boldsymbol{f_i}(j_f + 1) - f_i(j_f)) \tag{6}$$

Performance test curves based on which matrices were developed were characterized by constant pressure values for which the speed was changed. This allowed to create a simplified model using equation (7):

$$Q_b = 0.081 \cdot n - (0.72 \cdot p_c + 37.2) \tag{7}$$

The equation parameters were calculated using optimization methods. The task of minimizing the objective function was used, where the objective function was defined as the difference between the function sought and the matrix approach. Relative error was examined for characteristic pressure and flow points. The application of the simplified equation to the matrix approach generated an error in the range of 1% to 2%. The blowers are designed to work in the pressure range from 30 to 70 kPa, but the most common operating range is in the range of 45-65 kPa.

3.3 Pipeline

The pipeline has a large fluid flow capacity that significantly changes the dynamics of the model. Air capacity in the pipeline can be represented as:

$$C_c = k_c \cdot V_c \cdot p_c \tag{8}$$

where V_c determines the total volume of the pipeline (9), p_c determines the gas pressure inside the pipeline and kc is the unit conversion coefficient. The total volume is obtained as the sum of five pipeline fragments of different lengths and cross-sections using equation (10). Total volume:

$$V_c = V_1 + V_2 + V_3 + V_4 + V_5 \tag{9}$$

$$V_i = \pi \cdot \left(\frac{d_i}{2}\right)^2 \cdot l_i \, ; i \in \{1, 2, 3, 4, 5\} \tag{10}$$

The pressure change in the pipeline is achieved by using the principle of mass conservation in the pipeline node:

$$\frac{dp_c}{dt} = \frac{1}{C_c} \cdot (Q_b - Q_{air}) \tag{11}$$

The pressure losses occurring in the pipeline consist of three elements: unit linear pressure losses over a specified section, local pressure losses due to changes in pipe cross-sections, pressure loss due to height difference.

Unit linear pressure losses depend on the cross-section of the pipeline, as well as gas density and flow value. These changes were modelled according to the Renouard formula [16]:

$$\Delta p_R = 0{,}776457 \cdot 10^{-8} \cdot \rho \cdot \frac{V^{1,82}}{D^{4,82}} \tag{12}$$

where V is the mass airflow, D is the diameter of the pipeline and ρ is gas density. Individual gas constant for air r = 287,05 J/kgK and temperature was used to calculate the density:

$$\rho = p_c / r \cdot T \tag{13}$$

Local pressure losses are caused by the influence of the Reynolds number on the value of the local resistance coefficient ξ and gas flow speed w. They are described by equation (14) where ξ is presented as (15):

$$\Delta p_Z = \sum \xi_j \cdot \frac{\rho}{2} \cdot w^2 \quad j \in \{1, 2, 3, 4\} \tag{14}$$

$$\xi_j = \left(1 - \frac{A_j}{A_{j+1}}\right)^2 j \in \{1, 2, 3, 4\} \tag{15}$$

where A_j, A_{j+1} are pipe cross section areas before and after narrowing, respectively.

Pressure loss caused by the difference of levels significantly affect the pipelines with large changes in altitude and low gas pressures. The vertical sections influence the pressure change using the difference between the density of the medium, and air density under standard conditions ρ_p = 1.225 kg/m^3, according to the equation:

$$\Delta p_H = g \cdot \Delta H \cdot (\rho - \rho_p) \tag{16}$$

where g, ΔH are gravitational acceleration and height difference, respectively.

Due to small changes in height in the pipeline pressure loss caused by the difference of levels have not been used. The total pressure loss in the pipeline used in the model, visible in Fig. 2, can be represented as equation:

$$\Delta p_c = \Delta p_b - \Delta p_R - \Delta p_Z - \Delta p_h \tag{17}$$

3.4 Aeration segment units

The diffuser operation depends on the pressure difference (Δp_c) between the pipeline pressure (p_c) and the tank hydrostatic pressure drop (Δp_h) (see Fig. 2). The opening of the diffusers, i.e. the deflection of the membrane allowing air to escape, occurs when a minimum pressure p_{min} difference of 3.9 kPa is reached. In the steady-state the open diffuser airflow – pressure drop link is described by a nonlinear function:

$$Qair = \begin{cases} 0, & \Delta p_c < p_{min} \\ f\ (\Delta p_c), & \Delta p_c \geq p_{min} \end{cases} \tag{18}$$

The characteristic obtained from the manufacturer's data has been described by a nonlinear function and the diffuser airflow dynamics can be described as:

$$Qair = a_1 \cdot \Delta p_c^4 + a_2 \cdot \Delta p_c^3 + a_3 \cdot \Delta p_c^2 + a_4 \cdot \Delta p_c + a_5 \tag{19}$$

where $a_1 = -0.3484$, $a_2 = 7.1474$, $a_3 = 53.5072$, $a_4 = 178.1669$, $a_5 = -223.0322$. Function parameters were calculated using the least-squares method. The function has been simplified by approximating the first-order equation:

$$Qair = 5.167\Delta p_c - 19.6196 \tag{20}$$

Differences between the characteristics of the 1st and 4th order are shown in Fig. 3.

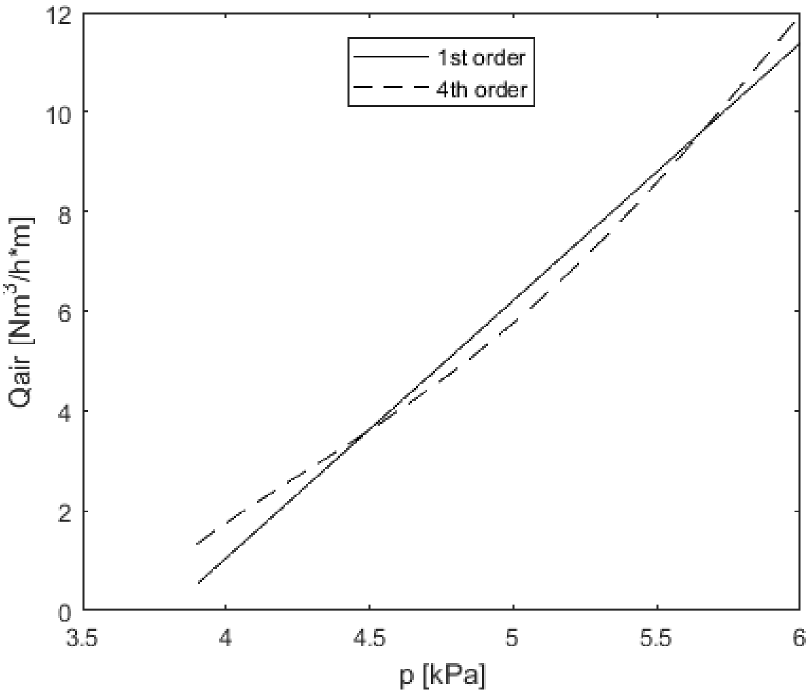

Fig. 3. Approximations of diffuser operation characteristics.

The hydrostatic pressure drop Δp_h is described in accordance with the expression:

$$\Delta p_h = \rho_m \cdot g \cdot h \tag{21}$$

where ρ_m, g, h are sewage density in the SBR tank, gravity acceleration and height of diffusers in SBR tank, respectively.

4 Verification test and results analysis

All values of model parameters are: d_1 = 104mm, d_2 = 84mm, d_3 = 154mm, d_4 = 69mm, d_5 = 80mm, l_1 = 75.6m, l_2 = 6m, l_3 = 13m, l_4 = 5.6m, l_5 = 5m, T = 20°C, g = 9.81 m/s^2, k_c = 1 m^2s^4/kg^2, r = 287,05 J/kgK, ρ_m = 1150 kg/m^3, p_{min} = 3.9 kPa, ρ_p = 1.225 kg/m^3, V_c = 1.2352 m^3. Model variable units: Q_{air} , Q_b, – Nm^3/hm; p_c, Δp_c , Δp_R, Δp_Z, Δp_H, Δp_h – kPa; n – rpm; h, ΔH – m, ρ – kg/m^3.

The pressure sensors available at WWTP Matowskie Pastwiska were used for the measurements. The blower control system sensors delivered measurements of pressure in pipeline (p_c) and blower frequency, which used to calculate the blower speed. Model validation tests were carried out on two SBR tanks with different filling levels and medium densities. This resulted in significant differences in hydrostatic pressure, and thus different pressures needed to open the diffusers. In the first SBR tank, the sewage level was 4.1 m, and the wastewater density was 2 g/l. In the second SBR tank, the wastewater level was 4.7 m and the wastewater density was 1.3 g/l. The measurement results were compared to the simulation results for the same conditions.

Comparing the operation of the blower in WWTP and the simulation tests of the model presented in the paper in Table 4 and Table 5, the small error results are about 1-2%.

Table 4. Simulation test of the first SBR tank

frequency [Hz]	blower [kPa]	model [kPa]	error [kPa]	absolute error
30	54.7	56.22	1.52	2.78%
35	55.1	56.34	1.24	2.25%
40	55.6	56.48	0.88	1.58%
45	56.0	56.61	0.61	1.09%
50	56.6	56.72	0.12	0.21%

Table 5. Simulation test of the second SBR tank

frequency [Hz]	blower [kPa]	model [kPa]	error [kPa]	absolute error
30	63.0	64.2	1.52	1.90%
35	63.6	64.7	1.24	1.73%
40	64.0	64.8	0.88	1.25%
45	64.9	65.0	0.61	0.15%
50	66.0	65.1	-0.9	-1.36%

The dynamics of blowers and diffusers are illustrated in Fig. 4. The characteristic moment of opening the diffusers after exceeding the pressure threshold is visible here.

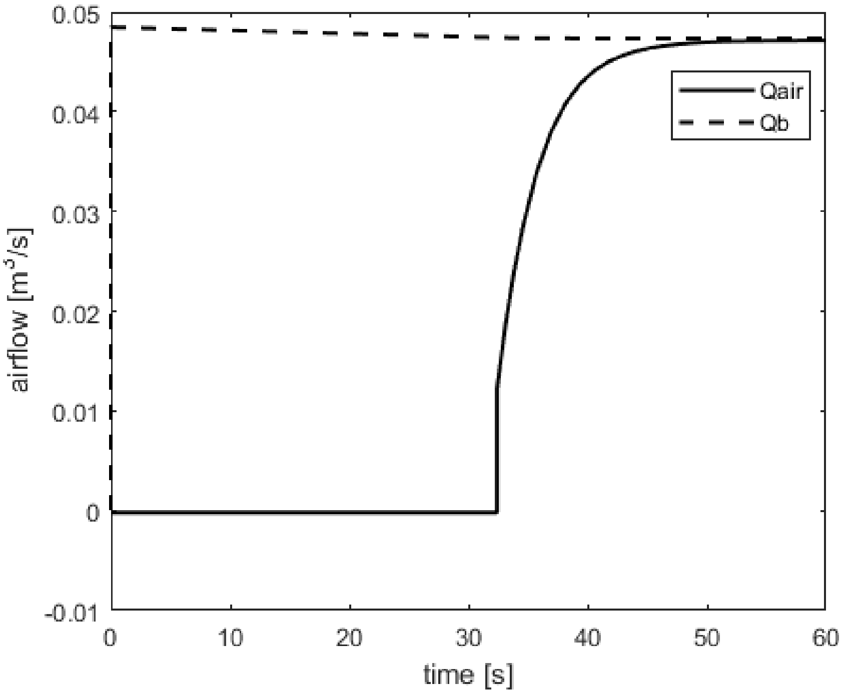

Fig. 4. Model airflows.

The characteristics of the effect of the SBR tank fill level on the Q_{air} at a constant blower speed is shown in Fig. 5. In the simulation test, the level of the medium varies from minimum to maximum while maintaining a constant density.

In summary, modelling results are verified to be satisfactory and can be used for control purposes.

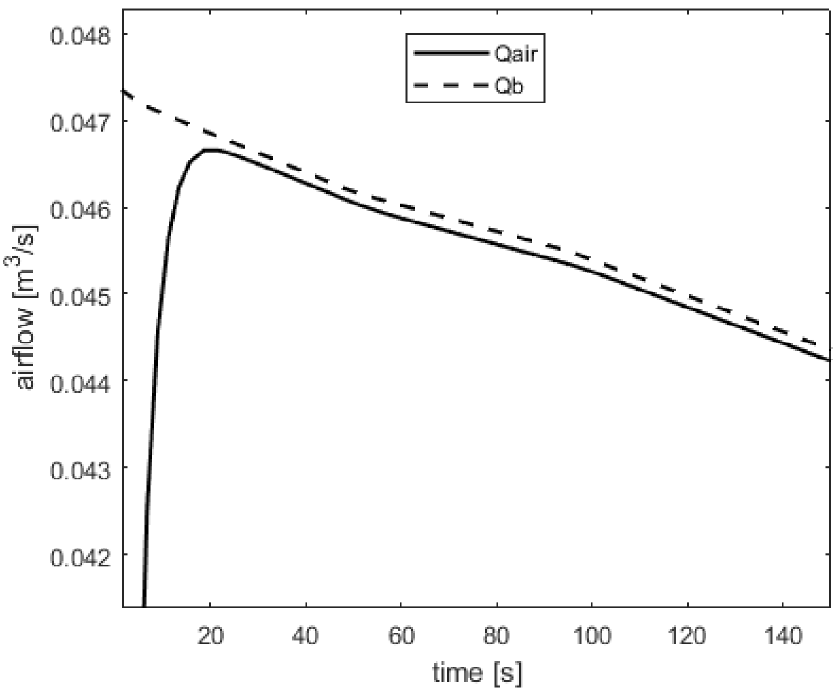

Fig. 5. Hydrostatic pressure test.

5 Conclusions

Aeration control systems are evolving towards the latest control solutions. More advanced control algorithms require mathematical models and simulations to work properly. This paper presents the modelling of the aeration system for control purposes. Relative to the previous research work [9], the diffuser approach has changed and equations describing pressure losses in the pipeline were used. The model structure, its parameterisation and approach to the parameter calculation from the manufacturer data have been successfully validated by application to the case study system.

Acknowledgements

The authors would like to thank the staff of the Matowskie Pastwiska WWTP for their help with access to the plant, information and data.

References

1. Wilderer P.A., Irvine R.L., Goronszy M.: *Sequencing Batch Reactor Technology*. Scientific and Technical Report No. 10, 2001, IWA Publishing, London.
2. Jenkins T.E.: *Aeration Control System Design. A Practical Guide to Energy and Process Optimization.* John Wiley&Sons, 2013, New Jersey.
3. Belchior C.A.C., Araújo R.A.M., Landeck J.A.C.: *Dissolved oxygen control of the activated sludge wastewater treatment process using stable adaptive fuzzy control*. Computers & Chemical Engineering 37(10), 2012, pp. 152-162.
4. Vrečko D., Hvala N., Stražar M.: *The application of model predictive control of ammonia nitrogen in an activated sludge process*. Water Science and Technology, Vol. 64, No. 5, 2011, pp. 1115-1121.
5. Åmand L., Carlsson B.: *Optimal aeration control in a nitrifying activated sludge process*. Water Research, Vol. 46, No. 7, 2012, pp. 2101-2110.
6. Błaszkiewicz K., Piotrowski R., Duzinkiewicz K.: *A Model-Based Improved Control of Dissolved Oxygen Concentration in Sequencing Wastewater Batch Reactor*. Studies in Informatics and Control,Vol. 23, No. 4, 2014, pp. 323-332.
7. Yang T., Qiu W., Ma Y., Chadli M., Zhang L.: *Fuzzy model-based predictive control of dissolved oxygen in activated sludge processes*. Neurocomputing, Vol. 136, 2014, pp. 88-95.
8. Piotrowski R.: *Two-Level Multivariable Control System of Dissolved Oxygen Tracking and Aeration System for Activated Sludge Processes*. Water Environment Research, Vol. 87, No. 1, 2015, pp. 3-13.
9. Piotrowski R., Skiba A.: *Nonlinear Fuzzy Control System for Dissolved Oxygen with Aeration System in Sequencing Batch Reactor*. Information Technology and Control, Vol. 44, No. 2, 2015, pp. 182-195.
10. Santín I., Pedret C., Vilanova R.: *Applying variable dissolved oxygen set point in a two level hierarchical control structure to a wastewater treatment process*. Journal of Process Control 28, 2015, pp. 40-55.
11. Piotrowski R., Błaszkiewicz K., Duzinkiewicz K.: *Analysis the Parameters of the Adaptive Controller for Quality Control of Dissolved Oxygen Concentration*. Information Technology and Control, Vol. 45, No. 1, 2016, pp. 42-51.
12. Jujun R., Chao Z., Ya L., Peiyi L., Zaizhi Y., Xiaohong Ch., Mingzhi H., Tao Z.: *Improving the efficiency of dissolved oxygen control using an on-line control system based on a genetic algorithm evolving FWNN software sensor.* Journal of Environmental Management, 187, 2017, pp. 550-559.
13. Du X., Wang J., Jegatheesan V., Shi G.: *Dissolved Oxygen Control in Activated Sludge Process Using a Neural Network-Based Adaptive PID Algorithm*. Applied Sciences, 8, 2018, 261.
14. Piotrowski R., Brdyś M.A., Konarczak K., Duzinkiewicz K., Chotkowski W.: *Hierarchical dissolved oxygen control for activated sludge processes*. Control Engineering Practice, Vol. 16, No. 1, 2008, 114-131.
15. Krawczyk W., Piotrowski R., Brdyś M.A., Chotkowski W.: *Modelling and identification of aeration systems for model predictive control of dissolved oxygen – Swarzewo wastewater treatment plant case study.* Conference: Proc. of the 10th IFAC Symposium on Computer Applications in Biotechnology, June 4–6, Cancun, Mexico, 2007.
16. Renouard M.P.: *Nouvelles règles à calcul pour la détermination des pertes de charge dans les conduites de gaz*. Journal des Usines à Gaz, October 1952, pp. 337-339.